Revista de Teledetección. 2007. 27: 5-16

Monitoring Weather and Climate with the Meteosat and Metop Satellites

J. Schmetz, D. Klaes, M. König and K. Holmlund

EUMETSAT. Am Kavalleriesand 31.D-64295 Darmstadt (Germany)
Johannes.Schmetz@eumetsat.int

RESUMEN

Este trabajo presenta una descripción del sistema de satélites meteorológicos gestionados por EUMETSAT. Comenzamos recordando la primera generación de satélites geoestacionarios europeos –satélites Meteosat–. Meteosat-1 fue lanzado en 1977. Desde entonces una serie de 7 satélites han estado proporcionando un servicio continuo de adquisición de imágenes en intervalos de media hora en tres bandas espectrales y Meteosat-7 es utilizado ahora para la observación del océano Índico. La llegada de la segunda generación de Meteosat (MSG) en 2002, renombrada a Meteosat-8 con el comienzo de las operaciones, marcó un salto importante en las capacidades de observación. Los satélites MSG captan imágenes en 12 bandas espectrales cada 15 minutos. Se presentan algunos ejemplos derivados de los datos MSG como observación de nubes, vectores de movimiento atmosférico y seguimiento de la inestabilidad, la cual presenta un gran potencial para pronosticar el inicio de la convección. Actualmente el sistema MSG dispone de un sistema dual, con Meteosat-9 como satélite principal y Meteosat-8 de apoyo proporcionando, ocasionalmente, servicios de gestión de imágenes en alta frecuencia. Finalmente, presentamos algunos resultados del primer satélite meteorológico de órbita polar de EUMETSAT, llamado Metop-A, lanzado en octubre de 2006. Metop proporciona observaciones avanzadas de perfiles de temperatura y humedad, vientos, ozono y gases traza. La instrumentación es un balance equilibrado entre la continuidad de instrumentos conocidos y nuevas técnicas utilizadas para la meteorología operacional; cabe destacar las observaciones térmicas hiperespectrales realizadas por IASI (Infrared Atmospheric Sounding Interferometer).

PALABRAS CLAVE: Meteosat, MSG, Metop.

ABSTRACT

The paper provides an overview of the meteorological satellite systems operated by EUMETSAT: We start by recalling the first generation of European geostationary Meteosat –satellites; Meteosat-1 was launched in 1977. Since then a series of seven satellites have been providing a continuous service acquiring half-hourly images in three spectral bands and Meteosat-7 is now used for observing the Indian Ocean area. The advent of the first Meteosat Second Generation (MSG) satellite in 2002, renamed to Meteosat-8 with the start of operations, marked a major step forward in terms of observing capability. MSG satellites take images in twelve spectral channels every 15 minutes. Examples of products derived with MSG data are shown such as cloud observations, atmospheric motion vectors and the instability monitoring which has great potential to forecast the onset of convection. The MSG system now features a dual satellite system with Meteosat-9 as prime satellite and Meteosat-8 providing stand by and occasional high frequency imaging services. Finally we present some results from the first polar orbiting meteorological satellite of EUMETSAT, named Metop-A, which was launched in October 2006. Metop provides advanced observations of temperature and humidity profiles, wind, ozone and trace gases. The instrumentation is a judicious balance between continuity of known instruments and novel techniques used for operational meteorology; notable are the hyperspectral thermal infrared observations with IASI (Infrared Atmospheric Sounding Interferometer).

KEY WORDS:Meteosat, MSG, Metop.

INTRODUCTION

Hasta Today we look back to more than 40 years of meteorological satellites that have proven to be the best way to observe the weather on large and regional scales. Typically, operational meteorology utilizes two types of satellites to provide the required information:

Low Earth Orbiting (LEO) satellites fly at relatively low altitudes of around 800 kilometres above Earth, mostly in polar (sun-synchronous) orbits, and can provide information with higher spatial

resolution. The whole surface of the Earth can be observed twice a day. More than one polar satellite, with different equatorial crossing times, is required for more frequent observations.

Geostationary satellites (GEO) are in the equatorial plane at an altitude of about 36,000 kilometres above Earth and have the same revolution time as the Earth itself and therefore always view the same area. They can perform frequent imaging and are ideal to observe rapidly changing phenomena like clouds and water vapour. The disadvantage of the geostationary orbit is the far distance from the surface/atmosphere system which puts stringent requirements on the signal-to-noise performance of the instruments.

EUMETSAT contributes to the global space-based observing system with both types of meteorological satellites namely the Meteosat series in geostationary orbit and the Metop satellites in a sun-synchronous polar orbit with an Equator crossing time at 0930UT.

FIRST GENERATION OF METEOSAT

The main instrument is a multispectral radiometer, which provides image data in three spectral bands:

- 0.5-0.9 μm visible band, 5.7–7.1 μm infrared water vapour (WV) absorption band, 10.5-12.5 μm thermal infrared window (IR) band.

Images of the full Earth disk are taken in the three spectral bands every half-hour. The radiometer scans the Earth from east to west by virtue of the spinning motion (100 rpm) of the satellite whilst the south to north scanning is achieved by stepping the radiometer through a small angle ($1{\cdot}25 \times 10^{-4}$rad) at each rotation of the satellite. There are two visible detectors (VIS1 and VIS2), that are placed in the focal plane of the primary telescope such that they observe adjacent lines of the Earth. Thus by combining each individual visible image, consisting of 2500 lines each of 5000 pixels, one obtains a visible image of 5000 lines of 5000 pixels with a sampling distance of 2.5 km at the subsatellite point (SSP). The subsatellite point sampling distance of the IR and WV images is 5 km, each image consisting of 2500 lines of 2500 pixels.

On the pre-operational satellites, i.e. Meteosat-1 through -3, the idea to include a water vapour (WV) channel occurred at a late stage in the development of the radiometer and was made possible by using the electronic chain of one of the visible channels. This meant that with the first three satellites two modes of operation were possible: Either mode 1 including VIS2, WV and IR or mode 2 with VIS1, VIS2 and IR. In practice during daylight hours the two modes were used alternately for successive slots whilst at night mode 1 was used exclusively. The VIS and WV images had a digitization of only 6 bits.

With the start of Meteosat-4 full resolution VIS and WV images could be obtained simultaneously and all image data were digitized with 8-bits. Noteworthy is also an improvement to the noise of the WV channel for Meteosat-4 through -7, which was a significant step toward the successful operational derivation of Atmospheric Motion Vectors (AMVs) in clear sky areas from WV images (Laurent, 1993). The clear-sky WV winds complemented the AMVs derived from the tracking of cloud features (Schmetz et al., 1993). Both became important in the assimilation of data for numerical weather prediction models.

METEOSAT SECOND GENERATION (MSG)

Like the first Meteosat series the MSG satellites (Schmetz et al., 2002) are spin-stabilized, however, capable of greatly enhanced Earth observations. The satellite's 12-channel imager, known as the spinning enhanced visible and infrared imager (SEVIRI), observes the full disk of the Earth with an unprecedented repeat cycle of 15 minutes in 12 spectral channels and improved spatial resolution (see Table 1). Meteosat-8 was launched in 2002 and Meteosat-9 followed in December 2005.

The MSG programme includes a series of four identical satellites, expected to provide observations and services over at least 15 years. Each satellite has an operating lifetime of seven years. As with the first Meteosat system, the new generation, starting with Meteosat-8, is planned as a dual-satellite service, with one additional satellite in orbit, primarily as back-up and useful for rapid scanning, i.e. a limited scan with a shorter repeat cycle.

Earth imaging with the second generation of Meteosat

The primary mission of the second-generation Meteosat satellites is the continuous observation of

the Earth's full disk with a multi-spectral imager. The repeat cycle of 15 minutes for full-disk imaging provides multi-spectral observations of rapidly changing phenomena such as deep convection. It also provides for better retrieval of wind fields, which are obtained from the tracking of clouds and water vapour features and gives unprecedented capabilities to detect preconvective instability and the change of cloud microphysics with time.

The imaging is performed by utilizing the combination of satellite rotation and scan mirror stepping. The images are taken from south to north and east to west. The eight thermal IR and three solar channels have a sampling distance of three kilometers at nadir and scan the full disk of the Earth. The high-resolution visible channel provides images with one kilometer sampling at nadir. Data rate limitations confine the high-resolution visible images to half the Earth in an east-west direction; however, the exact coverage of the Earth is programmable. The SEVIRI data have a 10-bit digitization and the radiometric performance of Meteosat-8 (see Schmetz et al., 2002) is excellent and exceeds the specification by far (Aminou et al. (2003).

Channel No.	Spectral Band (μm)	Characteristics of Spectral Band (μm) for Meteosat-8		
		λ_{cen}	λ_{min}	λ_{max}
1	VIS0.6	0.635	0.56	0.71
2	VIS0.8	0.81	0.74	0.88
3	NIR1.6	1.64	1.50	1.78
4	IR3.9	3.90	3.48	4.36
5	IR6.2	6.25	5.35	7.15
6	IR7.3	7.35	6.85	7.85
7	IR8.7	8.70	8.30	9.1
8	IR9.7	9.66	9.38	9.94
9	IR10.8	10.80	9.80	11.80
10	IR12.0	12.00	11.00	13.00
11	IR13.4	13.40	12.40	14.40
12	HRV	Broadband (0.4 – 1.1 μm)		

Table 1: Spectral characteristics of the spinning enhanced visible and infrared imager (SEVIRI) on Meteosat-8 in terms of central, minimum and maximum wavelength of the channels.

As an additional scientific payload, MSG satellites carry a geostationary Earth radiation budget (GERB) instrument (Harries et al., 2005) that observes the broadband thermal infrared and solar radiances exiting the Earth's atmosphere. GERB makes accurate measurements of the shortwave and longwave components of the radiation budget at the top of the atmosphere. GERB data are of interest for climatological studies and also for comparison with and validation of weather forecast models (Allan et al., 2005). As the first radiation budget experiment from geostationary orbit, the GERB instrument has great potential to shed new light on climate processes related to clouds, water vapour and aerosol (Slingo et al., 2006).

Products from Meteosat Second Generation

The application of the second generation of Meteosat satellites ranges from short-term forecasting to numerical weather prediction and climatological studies. Continuity for meteorological products from the first generation satellites is provided through products centrally derived at EUMETSAT. Those include inter alia atmospheric motion vectors (AMVs), cloud analysis, and atmospheric humidity. In addition there are novel products such as atmospheric instability and total ozone over the entire MSG field of view. In the following we describe three products and applications in more detail

Clouds

Information derived from cloud imagery such as cloud top height, cloud cover, cloud type, optical thickness, cloud phase (ice or water) and cloud microphysics is one of the key products of meteorological satellites. Cloud images observed in the visible and infrared parts of the spectrum are one element of the routine forecasts. The cloud images give a concise synoptic view of the weather systems and, animated as movie loops, they reveal the restless nature of the atmosphere on various spatial scales. Figure 1 shows an area around 0° and 25° E over Central Africa on 26 October 2006 around 12:15 UTC and is an example of the capability of Meteosat-8 to observe cloud microphysics by cleverly combining different spectral channels in a so-called RGB image; here red is assigned to the differences channel 5 minus channel 6; green: channel 4 minus channel 9 and blue: channel 3 minus channel 1 (channels are given in Table 1). Clouds tops that appear in yellow consist of small ice particles which in turn are indicative of strong convective activity (Rosenfeld and Lensky, 1998; Lensky and Rosenfeld, 2006). Figure 2 shows

the same area where pixels in red indicate cloud areas where the brightness temperature in the 6.2μm channel (channel 5) exceeds the one at 10.8μm (channel 9). We observe a close correspondence with the high level cloud areas with small ice particles indicating that areas of strong convection can also be observed by such a simple difference technique (e.g. Schmetz et al., 1997), which only takes the difference of channel 5 minus channel 9. An interesting aspect of such a simple product is the application to long-term data for climate studies. Potentially that could address the important question whether convective activity changes over decades. A prerequisite for this is a very accurate calibration which MSG satellites seem to offer.

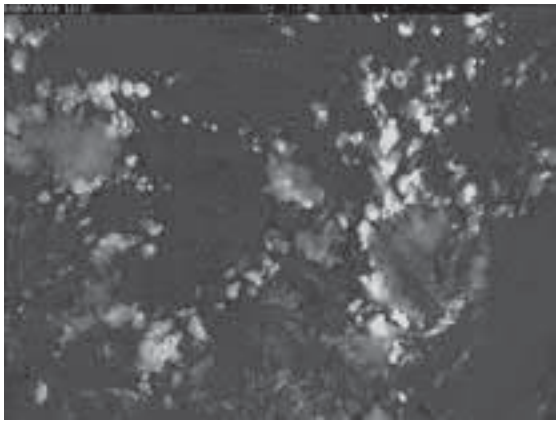

***Figure 1.** RGB image from Meteosat-8 over central Africa at 1215 UTC. Re: chl 5minus chl 6; green: chl 4 minus chl 9; Blue: chl 3 minus chl1. Clouds appearing yellow are areas of strong convection.

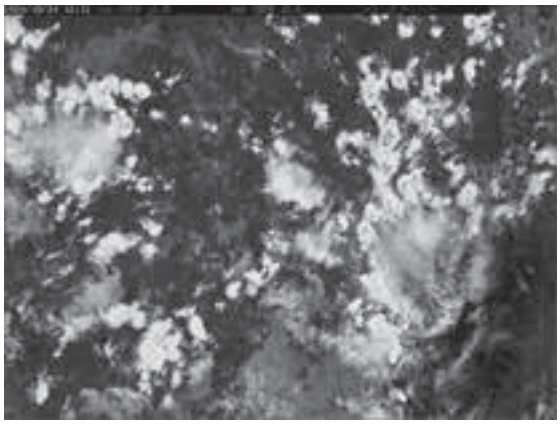

***Figure 2.** Meteosat-8 channel 9 image for the same area as Figure 1. Red corresponds to areas where the brightness temperature of chl 5 is warmer than chl 9.

Global Instability Index (GII)

Convective systems often develop in thermodynamically unstable airmasses. As the convective s systems have the potential to develop into severe storms, it is of high interest to identify storm potential while the system is still in a pre-convective state. A number of instability indices have been defined to describe such situations. Traditionally, these indices are taken from temperature and humidity soundings by radiosondes. As radiosondes are only of very limited temporal and spatial resolution there is a demand for satellite-derived indices. The GII product consists of a set of indices which describe the layer stability of the atmosphere. It comprises four classic instability indices: i) the Lifted Index, ii) the K Index, iii) the KO Index, iv) the Maximum Buoyancy Index. The total precipitable water is added as a fifth index describing the airmass.

The retrieval of these parameters from satellite data is only possible under cloud-free conditions. Figure 3 depicts the Global Instability Index (GII) (König, 2002) derived over Europe for 30 July 2006. It is an example of the Lifted Index, retrieved over 3x3 pixel areas, where negative values are indicative of potential instability. The region over central eastern Europe was on this particular day characterised by an unstable airmass, shown in yellow and red colours. White areas are clouds or the region outside the processing area.

Figure 4 is the IR window image at 1200 UTC (left panel) and at 1800 UTC (right panel), respectively. The midday image is basically cloud-free in the regions that are indicated as unstable in Figure 3. In the late afternoon at 1800 UTC we observe a strong storm activity. This example nicely depicts a case where instability indices, as they are derived in the GII product, are useful to anticipate the onset of strong convection.

Atmospheric Motion Vectors

Winds in terms of atmospheric motion vectors (AMVs) are the most important product from geostationary satellites for Numerical Weather Prediction (NWP) models. They are generated operationally by all of the operators of geostationary meteorological satellites for more than two decades. Figure 5 shows an example of AMVs derived

Todas las figuras precedidas de asterisco se incluyen en el cuadernillo anexo de color

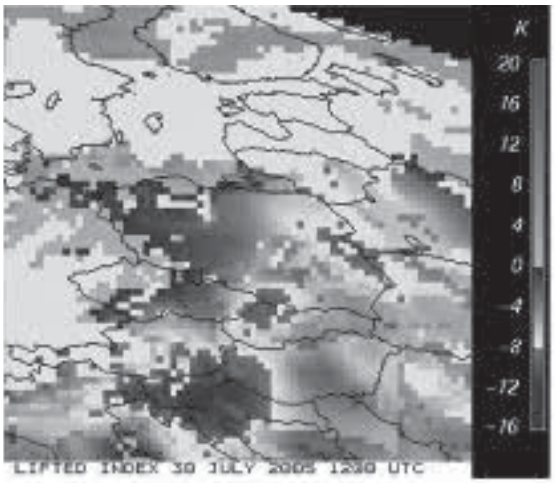

***Figure 3.** Lifted index computed from Meteosat-8 radiances for 30 July 2006 at 1200 UTC over central, Eastern Europe. Yellow and red indicates areas with instable airmass.

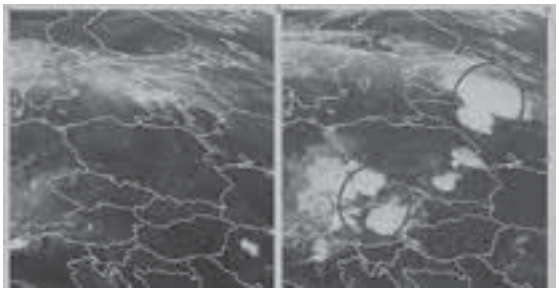

Figure 4. Meteosat-8 channel 9 images corresponding to the area in Figure 3. Left panel at 1200 UTC and right panel at 1800 UTC when strong convective system had formed.

from Meteosat-8 channel 9 images by tracking cloud features. The method of deriving a wind vector is in principle quite simple: cloud or water vapour features are tracked from one image to the next, thereby measuring a displacement vector. Assuming that the displacement vector represents a wind and assigning the vector to the correct height, one obtains a wind vector. The basic technique can be applied to clouds in both infrared and visible satellite imagery, as well as to other tracers, such as the patterns of atmospheric water vapour. There are obvious limitations of AMVs, for instance: the wind blows through some stationary clouds generated by mountains, clouds grow or dissipate as they move. Thus clouds are not generally good passive tracers; the same is true for water vapour features. Therefore good target selection is important. Very

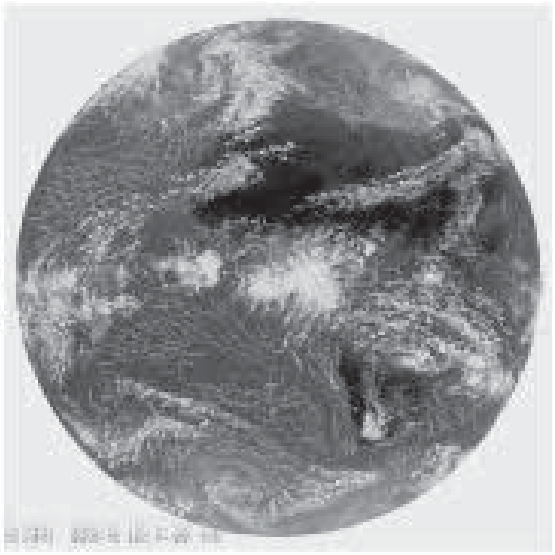

***Figure 5.** Examle of an Atmospheric Motion Vector (AMV) product from Meteosat-8 for 23 February 2003. Different colours correspond to different altitudes

difficult is also the height assignment of the displacement vectors, which often necessitates multispectral techniques (Nieman et al., 1993). And last but not least quality control is essential in order to produce good AMV products (Holmlund, 1998).

The importance of satellite data for Numerical Weather Prediction has grown steadily over the last two decades and nowadays satellite data are the most important data for NWP (Kelly and Thépaut, 2006). In recent studies ECMWF (European Centre for Medium Range Weather Forecasts) investigated the relative contributions of the various space observing systems within the ECMWF data assimilation system. The Observing System Experiment studies (OSE) assumed the current full conventional observing system as baseline, consisting of radiosondes, aircraft data, profiler networks, surface land data, buoy observations and ship data. Individual satellite data were then added sequentially.

Figures 6 and Figure 7 show the correlation forecasts from ECMWF and observed anomalies of the 500 hPa height fields. Forecasting these anomalies accurately is important in weather forecasting. The higher the correlation the better the forecast. Forecast with correlations above 60% are generally considered useful. Figures 6 and Figure 7 give those anomaly correlations over six days for the Northern latitudes (20°N - 90°N) and Southern latitudes (20°S - 90°S), respectively. The red curve shows

Todas las figuras precedidas de asterisco se incluyen en el cuadernillo anexo de color

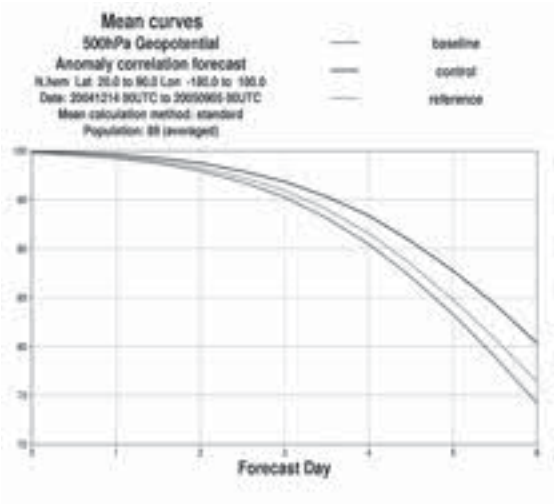

***Figure 6.** Correlation of the observed and forecast anomalies of 500 hPa geopotential heights in the ECMWF forecast system for forecasts up to 6 days. This figure shows Northern latitudes from 20° N - 90° N. Different curves pertain to utilization of different observation; black: all observation; red: only conventional (non-satellite) observations; orange: conventional plus Atmospheric Motion Vectors (AMVs).

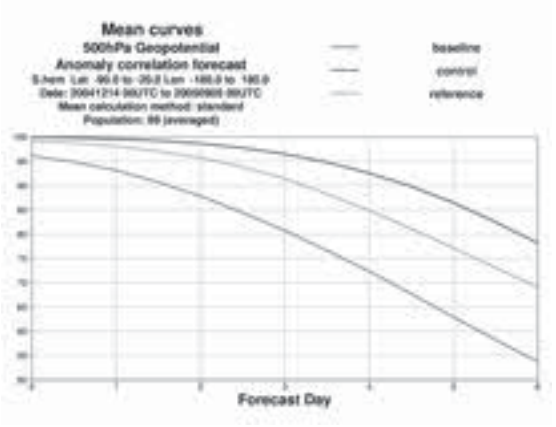

***Figure 7.** As Figure 6 except for Southern latitudes 20° S – 90° S.

the baseline defined above and the black curve the control forecast which includes all data. The orange line is the baseline including as additional satellite data the Atmospheric Motion Vectors (AMVs) from all geostationary satellites and also the AMVs over polar regions from the MODIS instrument (Key et al., 2003). It is interesting to see that over the Northern hemisphere the forecast gets improved by several hours thanks to the AMV data; over the data sparse Southern hemisphere the improvement is as large as about 1.5 days. In order to understand the relative contribution of the AMVs it is important to note that in a full data assimilation study the positive increment due to AMVs is much smaller; i.e. there is redundancy between the data and therefore the first data in system do have the highest impact (Kelly and Thépaut, 2006).

Other products

Over and above the central processing at EUMETSAT, there are products from a geographically distributed network of services, Satellite Application Facilities (SAF), hosted by National Meteorological Services and other institutions. SAFs include the processing of Metop data too (see chapter 4). The idea behind the network of SAFs is that more products from MSG (and also from the future EUMETSAT Polar System) can be derived effectively capitalizing on the scientific expertise across the EUMETSAT Member States. There are seven SAFs addressing seven themes: i) Ocean and Sea Ice hosted by Météo-France, ii) Numerical Weather Prediction hosted by the MetOffice, UK, iii) Nowcasting hosted by the Institute for Meteorology, Spain; iv) GRAS Meteorology hosted by the Danish Meteorological Institute, v) Land Surface Analysis hosted by the Portuguese Meteorological Institute, vi) Climate Monitoring hosted by the German Met Service (DWD), vii) Ozone and Atmospheric Chemistry Monitoring hosted by the Finnish Meteorological Institute. An eighth SAF on Hydrology is being developed. Each SAF is provides operational services to end-users, including real-time and/or off-line product services, distribution of user software packages, and data management (for details see www.eumetsat.int). More recently other products emerged that provide important information on other aspects of earth-atmosphere system such as fire monitoring (Calle et al., 2006).

THE EUMETSAT POLAR SYSTEM (EPS)/METOP

Overview

The first satellite of the EUMETSAT Polar System (EPS), called Metop series, was launched in October 2006. Metop-A provides advanced observations of temperature and humidity profiles, wind, ozone and other trace gases. The instrumentation of

Metop is a judicious balance between continuity of known instruments and novel observations, notably the hyperspectral thermal infrared observations with an interferometer and radio occultation measurements. Metop satellites are also the European contribution to the space-based global observing system and to the joint European/US operational polar satellite system. Metop covers the mid-morning (9:30) orbit, whereas the US continues to cover the afternoon orbit. The three Metop satellites are expected to provide services for at least fourteen years. A detailed description is provided by Klaes et al. (2007).

With eight instruments taking observations of the earth-atmosphere system, Metop provides both continuity to previous operational measurements and also progress through data from novel instruments. AVHRR (Advanced Very High Resolution Radiometer), and the Advanced TIROS (Television and Infrared Operational Satellite) Operational Vertical Sounder (ATOVS) package, composed of HIRS/4 (High Resolution Infrared Radiation Sounder), AMSU-A (Advanced Microwave Sounding Unit - A) and MHS (Microwave Humidity Sounder) provide the continuity to the current NOAA POES (NOAA-KLM or NOAA-15, 16, 17) system (where ATOVS is composed of HIRS/3, AMSU-A and AMSU-B) and are common to the payload on the afternoon satellites (NOAA-18 and NOAA-N'). MHS is a EUMETSAT development and replaced the AMSU-B instrument in the ATOVS suite, while NOAA provides the AMSU-A, HIRS/4 and AVHRR instruments. MHS is already in space since the launch of NOAA-18 in May 2005.

The IASI (Infrared Atmospheric Sounding Interferometer) instrument is novel technology, developed by CNES, and introduces hyperspectral resolution sounding capabilities in the infrared (Hébert et al., 2004).

Some payload components have been developed from the heritage of proven research missions of the European Space Agency (ESA). One of these components is GOME-2 (Global Ozone Monitoring Experiment) building on the heritage of GOME-1, another one is the ASCAT (Advanced Scatterometer), which draws on the ERS active microwave instrument (AMI) heritage.

The impact of radio-occultation measurements like GRAS (GNSS Receiver for Atmospheric Sounding, Luntama, 2001), has been successfully demonstrated through impact studies in Numerical Weather Prediction (Collard and Healy, 2003).

ATOVS - Continuity

Continuity is an important aspect to operational services. For nearly two decades the information on temperature and humidity soundings and surface information (including clouds) for numerical weather prediction and other applications, has been provided by the ATOVS suite supported by the AVHRR imager for both morning and afternoon missions, on the NOAA satellites. The instrument suite is common to the two components of the Initial Joint Polar System (IJPS), i.e. Metop-A and the future Metop-B (AM satellites) and NOAA-18 and the future NOAA-N' (PM satellites). It consists of four instruments, three of which are provided by NOAA.

i) the High Resolution Infrared Radiation Sounder (HIRS/4) measures temperature and humidity of the global atmosphere in cloud-free or partly cloudy conditions and is or will be on Metop-A and -B. HIRS/4 is a filter-wheel radiometer, which measures radiances in 19 infrared channels, and one additional channel in the visible. An important improvement to HIRS/4 is the 10 km IFOV (Instantaneous Field of View) in contrast to the 20 km IFOV of the previous HIRS version.

ii) The Advanced Microwave Sounding Unit-A (AMSU-A) measures the temperature of the global atmosphere in nearly all weather conditions. AMSU-A provides microwave atmospheric measurements in 15 channels between 23.8 GHz and 89 GHz mainly for temperature sounding.

iii) The Microwave Humidity Sounder (MHS) provides atmospheric measurements in five microwave channels for humidity measurements. MHS has been developed under EUMETSAT responsibility and replaces the previous generation AMSU-B microwave humidity sounder. MHS has been flying on NOAA-18 –which is the first component of the IJPS (Initial Joint Polar System) in space– since May 2005.

iv) The Advanced Very High Resolution Radiometer (AVHRR/3) is a six channel imager and provides globally visible, near infrared and infrared imagery of clouds, the ocean and land surface. The AVHRR data on Metop are provided globally at the full resolution, i.e.1.1 km at nadir.

IASI - New Technology

The Infrared Atmospheric Sounding Interferometer (IASI) introduces a new technology to operatio-

nal satellite observation. The purpose of IASI is to measure temperature, water vapour and trace gases at a global scale. The measurement principle is based on Michelson interferometry providing 8461 spectral channels, aligned in three bands between 3.62 μm (2760 cm-1) and 15.5 μm (645 cm-1). The unapodised resolution is between 0.3 and 0.4 cm-1, with a spectral sampling of 0.25 cm-1. IASI samples the earth-atmosphere system with instantaneous fields of views (IFOV) of 12 km at nadir and a sampling distance around 25 km.

Included in the IASI instrument is an Integrated Imaging System (IIS). It is used to provide the Earth location of the IASI pixels at 1 km accuracy through co-registration with the AVHRR pixels during the Level 1 processing. The mapped AVHRR information will then be used to classify inhomogeneous IASI scenes (Phillips and Schlüssel, 2005) and to determine the cloud coverage of an IASI pixel. The IIS consists of a broadband radiometer measuring between 10 and 12 μm.

IASI data will be used in synergy with the microwave sounding instruments to which the scan is synchronized. Products will include, besides Level 1 radiance spectra, vertical profiles of temperature, humidity and ozone at global scale. The envisaged accuracy is 1 K per 1 km layer which can be achieved throughout most of the troposphere and lower stratosphere.

ASCAT and GOME –2 – Operational Use of Research Missions

Two instruments on Metop have a heritage to missions on the ESA Earth Remote Sensing (ERS) Satellites, namely the Advanced Scatterometer (ASCAT) and the Global Ozone Monitoring Experiment (GOME-2).

i) Advanced Scatterometer (ASCAT) provides near-surface wind speed and direction over the global oceans. ASCAT is a real aperture, vertically polarized C-band radar. ASCAT doubles the coverage of the surface (compared to the earlier instrument on ERS) with two swaths of measurements, one on each side of the sub-satellite track.

Six ASCAT antennas illuminate the surface sequentially with pulses at a carrier frequency of 5.225 GHz. The backscatter signal is measured to determine the Bragg scattering from the sea surface. Wind speed and direction are estimated using a model, which relates them to the normalised radar backscattering cross section (σ_0). The data are collected from three azimuth angles (45º, 90º and 135°) across both of the 550-km wide swaths on both sides of the nadir track. ASCAT provides ocean surface winds at 50 km resolution over a 25 x 25 km^2 grid along and across both swaths. In addition a high-resolution wind product is generated at 25-km horizontal resolution on a 12.5 x 12.5 km^2 grid.

ii) Global Ozone Monitoring Experiment (GOME-2) provides the possibility to monitor the Ozone total column and profiles and components related to Ozone chemistry in the Earth's atmosphere. The instrument on Metop profits from experience gained over many years of observation and data analysis with the GOME-1 instrument on ERS-2. GOME-2 has an increased spatial sampling of 40 x 40 km2 , an increased Earth coverage due to increased swath width (1920 km), improved polarisation measurements (12 bands), enhanced onboard calibration through added white light source and increased spectral sampling.

GOME-2 measures the backscattered UV-VIS radiation in four bands between 240 and 790 nm, at a spectral resolution between 0.25 and 0.5 nm. The accuracy of Ozone total column and profiles is better than 5% and 15% above 3o hPa and better than 50% below 30 hPa respectively. The objective is 3% for columns and 10% for profiles at all levels. Additional intended products are vertical columns of BrO, OClO, NO2 and SO2, expected to be retrieved with accuracy better than 20%.

GNSS Receiver for Atmospheric Sounding (GRAS)

GRAS measures the temperature of the upper troposphere and in the stratosphere with high vertical resolution in all weather conditions and potentially measures humidity in the troposphere (Luntama, 2001). GRAS makes use of the GPS (Global Positioning System) satellite constellation. An occultation occurs for GRAS whenever a GPS satellite rises or sets over the horizon as observed by Metop and the ray path from its transmitter traverses the Earth's atmospheric limb. The bending angle attributable to this ray contains information on the refractivity and thereby on temperature and humidity. With the nominal 24 GPS satellites, a single GRAS instrument in near polar orbit at 824 km will observe over 500 occultations per day, distributed quite uniformly over the globe.

Examples of Metop Products

Operational meteorology comprises a wide range of activities, related to the analysis and prediction of the changing weather elements in time. Operational satellites can provide the necessary long term monitoring capabilities and thus contribute to the detection and documentation of climate change. Many requirements for climate monitoring coincide with or overlap with the mission requirements for operational meteorology. The polar orbit is the obvious choice for climate monitoring because one system observes the full globe.

IASI Radiances

IASI, the most innovative instrument on Metop, provides hyperspectral sounding resolution and high vertical resolution required by global NWP. It will provide global measurements of temperature and water vapor with unprecedented accuracy (1 K at 1 km vertical resolution, 10% Relative Humidity). In addition, greenhouse gases such as ozone, nitrous oxide, carbon dioxide, and methane will be retrieved and will contribute to environmental change monitoring (Turquety et al., 2004). Furthermore surface temperature, surface emissivity, and cloud characteristics will be retrieved from IASI data. The Atmospheric Infrared Sounder (AIRS) on NASA's AQUA satellite has demonstrated the capabilities of hyperspectral infrared sounders and their impact for numerical weather prediction and greenhouse gas monitoring (Chahine et al., 2006, Le Marshall et al., 2006). The accuracy and the performance of the IASI retrievals have been demonstrated with data from AIRS (Atmospheric Infrared Sounder) instrument. (Calbet and Schlüssel, 2006). Figure 8 shows the high-resolution spectra in terms of equivalent brightness temperature from the IASI hyperspectral sounder for tropical (red), mid latitude (green) and a cold arctic (blue) atmospheres, respectively. Measurements at such high spectral resolution (more than 8000 channels) provide the basis for resolving the vertical structure of temperature and humidity in an unprecedented way and also offer unique opportunities for climate monitoring.

MHS Radiances

Sounder level 1 products provide Earth located radiances on the original measurement grid.

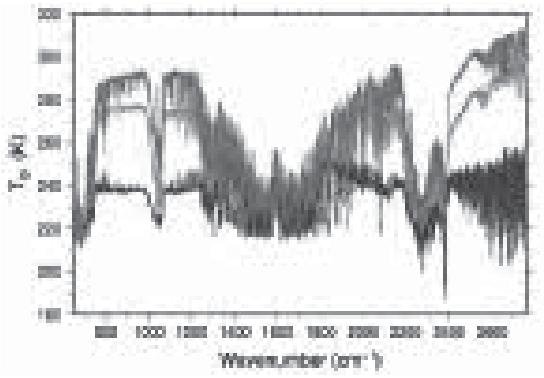

***Figure 8.** Spectra in terms of equivalent brightness temperature from the IASI hyperspectral sounder for tropical (red), mid latitude (green) and a cold arctic (blue) atmospheres, respectively.

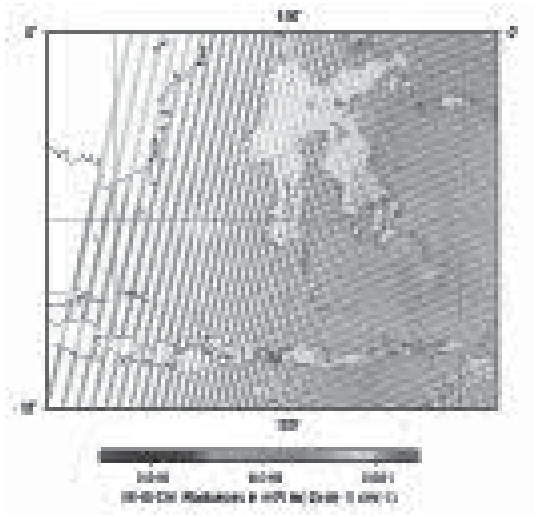

***Figure 9.** Radiances at 89 GHz (channel 1) from the Microwave Humidity Sounder (MHS) over indonesian Islands and Borneo (upper left).

Figure 9 displays an example for MHS channel-1 (at 89 GHz) radiances for a Metop descending pass over Indonesia. Besides the radiance values the image shows the good geolocation inferred from the comparison between the MHS channel-1 radiances and the coastlines. The geolocation has sufficient accuracy for further derivation of higher-level ATOVS products. As the MHS channel-1 is a window channel it depicts surface characteristics.

Ocean Surface Winds

Atmospheric winds are an important parameter in numerical weather prediction. Wind contains infor-

Todas las figuras precedidas de asterisco se incluyen en el cuadernillo anexo de color

mation about the atmospheric mass field and hence temperature advection. Scatterometer observations provide surface wind vectors over the oceans, where conventional observations are sparse. On ground the ASCAT signals are processed to obtain normalised backscatter measurements, resulting in 21 nodes per swath (42 in total) for the 50-km resolution winds, and 42 nodes per swath (84 in total) for the 25-km resolution winds. The aim is to measure the ocean wind field at the ocean surface at an accuracy of 10% in the wind speed components and 20% in the direction.

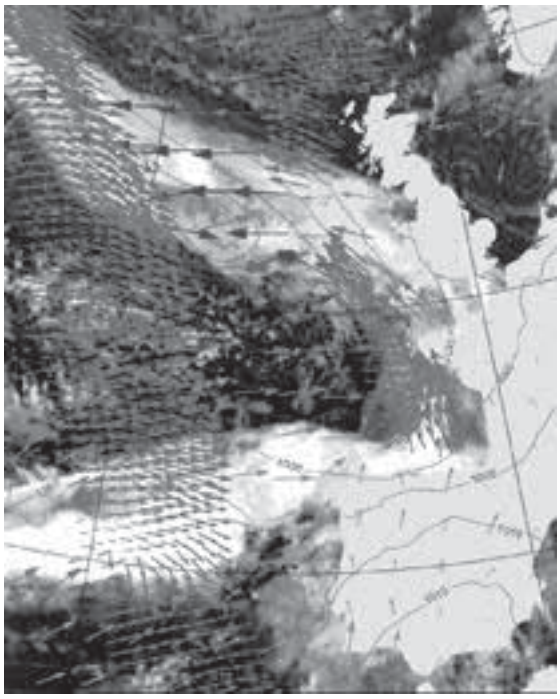

***Figure 10.** ASCAT winds over the Atlantic on 12 February 2007, around 21 UTC (red arrows). The picture shows only every second ASCAT wind vectors, with 25-km spacing. The blue and purple arrows show a 3-hour forecast of winds from the KNMI High-Resolution Limited Area Model (HiRLAM). In the background, a METEOSAT infrared image is shown in black and white (KNMI, 2007)

Fig. 10 shows an example of ocean wind vectors, retrieved from early pre-calibrated ASCAT data (KNMI and ECMWF, 2006).

Further potential of ASCAT lies in the measurement of sea ice boundaries and sea ice concentration and type (e.g. Cavanié et al., 1997). Other emerging applications are related to land surface observations; e.g. soil moisture (Wagner et al, 2003).

SUMMARY AND OUTLOOK

The European geostationary Meteosat satellites have been a great success and are, nowadays, considered as indispensable for meteorological services. Seven Meteosat's of the first generation provided operational services since 1977, imaging the full disk of the Earth every 30 minutes in three spectral bands. With Meteosat-8 a new series of geostationary satellites has started. After the launch end of August 2002 an extended commissioning period ended with the start of operations in January 2004. The established services from the first-generation satellites did continue with a seamless transfer to operations. Meteosat-9 was launched in December 2005 and both now offer a wealth of new observational capabilities. SEVIRI, the operational imager, has twelve spectral channels and observes the Earth (full disk) every 15 minutes. The multispectral imaging and the high temporal repeat cycle benefit weather forecasting and will improve severe weather warning. Significant benefits will come through the assimilation of products in numerical weather models and through improved Nowcasting applications (e.g. Menzel et al., 1998). Four Meteosat satellites of the second generation are foreseen to cover operational services at least until 2015. Then the Meteosat third generation is expected to take over.

The new EUMETSAT Polar System (EPS) with the Metop satellites, developed jointly with the European Space Agency (ESA) and CNES, and saw its first launch in October 2006. It establishes the European contribution to the global polar meteorological space observing capabilities. The Metop satellites EPS form together with the NOAA (and in the future the NPOESS (National Polar Orbiting Environmental Satellite System)) satellites a joint polar system, with Metop serving the morning orbit around 0930h and the US satellites the 1330h Equator crossing time. Metop provides on the one hand continuity to current systems, through continuation of the proven ATOVS instrument suite and the AVHRR imager, on the other hand it includes novel capabilities, i.e.: i) IASI provides high spectral resolution sounding and radiances which will improve NWP and has good potential for climate monitoring because of its high spectral resolution, good calibration and good instrument characterisation; ii) Instruments with heritage from ESA Earth observation missions (ASCAT and GOME) are utilised operationally and provide sea surface winds

Todas las figuras precedidas de asterisco se incluyen en el cuadernillo anexo de color

and ozone, aerosol and trace gases, respectively. iii) With GRAS the radio occultation principle is introduced for the first time into an operational system and demonstrates the capability to provide high quality soundings in near real time from radiooccultation.

The Metop satellites cover 14 years of operations and assure long-term and consistent observations that provide a sustained basis for improved utilization in NWP. Furthermore it provides the basis for climate-monitoring which will be enhanced through a regular reprocessing of data and products based on advances in the scientific understanding.

For details on instruments and general information the reader is referred to: www.eumetsat.int

REFERENCES

ALLAN R. P., A. SLINGO, S.F. MILTON and I. CULVERWELL 2005: Exploitation of Geostationary Earth Radiation Budget data using simulations from a numerical weather prediction model: Methodology and data validation. J. Geo. Res., 110, D14111, doi: 10.1029/2004JD005698

AMINOU, D. et al., 2003: Meteosat Second Generation: A comparison of on-ground and on-flight imaging and radiometric performances of SEVIRI on MSG-1, Proceedings of 'The 2003 EUMETSAT Meteorological Satellite Conference', Weimar, Germany, 29 September-3 October 2003, p. 236-243.

CALBET, X, P. SCHLÜSSEL, T. HULTBERG, P. Phillips, and T. August, 2006: Validation of the operational IASI Level 2 processor using AIRS and ECMWF data. Advances in Space Research, Vol. 37, No. 12, pp. 2299-2305.

CALLE, A. J. L. CASANOVA and A. ROMO, 2006: Fire detection and monitoring using MSG Spinning Enhanced Visible and Infrared Imager (SEVIRI) data, J. Geophys. Res., Vol. 111, G04S06, doi:10.1029/2005JG000116.

CAVANIÉ, A., R. EZRATY and F. GOHIN, 1997: Sea ice monitoring. In: Land Surface Observations using the ERS Wind scatterometers. Institute for Applied Remote Sensing, Wedel, Germany, 4-6.

CHAHINE, M. and CO-AUTHORS, 2006: AIRS Improving Weather Forecasting and Providing New Data on Greenhouse Gases. Bull. Amer. Met. Soc., Vol. 87, No. 7, pp. 911-926.

COLLARD, A and S. HEALY, 2003: The combined impact of future space-based atmospheric sounding instruments on numerical weather prediction analysis fields: A simulation study. Q. J. R. Meteorol. Soc., 129, 2741-2760.

HARRIES J.E. et al. (2005) The Geostationary Earth Radiation Budget Project. Bull. Am. Meteorol. Soc., 86, 945-960

HÉBERT, P., D. BLUMSTEIN, C. BUIL, T. CARLIER, G. CHALON, P. ASTRUC, A. CLAUSS, D. SIMÉONI, B. OURNIER, 2004: IASI Instrument: technical description and Measured Performances. Proceedings of the 5th International Conference on Space Optics (ICSO 2004), 30 March –2 April 2004, Toulouse, 49-56.

HOLMLUND, K., 1998: The utilization of statistical properties of satellite-derived atmospheric motion vectors to derive quality indicators. Wea. and Forecasting. 13, 1093-1104.

KELLY, G. and J.N. THÉPAUT (2006) Observing System Experiments in support of EUCOS. Presentation to the 21st EUMETSAT STG Science Working Group, September 2006.

KEY, J., J.R., D. SANTEK, C.S. VELDEN, N. BORMANN, J.N. THÉPAUT, L.P. RIISHOJGAARD, Y. ZHU and W.P. MENZEL (2003) Cloud-Drift and Water Vapor Winds in the Polar Regions from MODIS, IEEE Transactions on Geoscience and Remote Sensing 41, pp. 482-492.

KLAES, K. D., M. COHEN, Y. BUHLER, P. SCHLÜSSEL, R. MUNRO, J-P LUNTAMA, A.VON ENGELN, E. Ó CLÉRIGH, H. BONEKAMP, J. ACKERMANN, J. SCHMETZ, 2007: An Introduction to the UMETSAT Polar System (EPS/MetOp). Accepted by Bull. Amer. Met. Soc.

KÖNIG, M., 2002: Atmospheric instability parameters derived from MSG SEVIRI observations. Technical Memorandum No. 9, EUMETSAT Programme Development Department, pp. 27.

LAURENT, H., 1993: Wind extraction from Meteosat water vapour channel image data. J. Appl. Meteorology, 32, 1124-1133.

LEMARSHAL, J., and CO-AUTHORS, 2006: Improving Global Analysis and Forecasting with AIRS. ull. Amer. Met. Soc., Vol. 87, No. 7, pp. 891-894.

LENSKY, I.M. and D. ROSENFELD, 2006: The time-space exchangeability of satellite retrieved relations between cloud top temperature and

particle effective radius. Atmos. Chem. Phys., 6, 2887-2894.

LUNTAMA, J-P. 2001. EPS GRAS mission for operational GPS Meteorology. Proceedings of the 14th International Technical Meeting of the Satellite Navigation of The Institute of Navigation, ION GPS 2001, Salt Lake City, Utah. Sept. 11-14, 2001.

MECIKALSKI, J. and K. BEDKA, 2006: Forecasting convective initiation by monitoring the evolution of moving cumulus in daytime GOES imagery. Mon. Wea. Rev., 134, 49-78.

MENZEL, J. M., F. C. HOLT, T. J. SCHMIT, R. M. AUNE, A. J. SCHREINER, and D. G. GRAY, 1998: Application of GOES-8/9 soundings to weather forecasting and nowcasting. Bull. Amer. Meteor. Soc., 79, 2059-2077.

PHILLIPS, P. and P. SCHLÜSSEL, 2005: Cassification of IASI inhomogeneous scenes using colocated AVHRR data. Proceedings SPIE the International Society for Optical Engineering. Remote Sensing of Clouds and the atmosphere X Vol. 5979, pp. 29-41.

ROSENFELD, D. and I.M. LENSKY, 1998: Satellite-based insights into precipitation formation processes in continental and maritime convective clouds, Bull. Amer. Meteor. Socl, 79, 2457-2476.

SCHLÜSSEL, P. and M. GOLDBERG, 2002: Retrieval of Atmospheric Temperature and Water Vapour from IASI Measurements in partly cloudy situations. Adv. Space Res., Vol. 29, No. 11, 1703-2706.

SCHMETZ, J., K. HOLMLUND, J. HOFFMAN, B. STRAUSS, B. MASON, V. GAERTNER, A. KOCH and L. VAN DE BERG, 1993: Operational cloud motion winds from METEOSAT infrared images, J. Appl. Meteorology, 32, 1206 1225.

SCHMETZ, J., S.A. TJEMKES, M. GUBE, and L. VAN DE BERG, 1997: Monitoring deep convection and convective overshooting with METOSAT. Adv. Space Res., 19, 433-441.

SCHMETZ, J., P. PILI, S. A. TJEMKES, D. JUST, J. KERKMANN, S. ROTA and A. RATIER, 2002: An Introduction to Meteosat Second Generation (MSG). Bull. Amer. Meteor. Soc., 83, 977-992.

SLINGO, A. et al., 2006: Observations of the impact of a major Saharan dust storm on the atmospheric radiation balance. Geo. Res. Let., Vol. 33, L24817, doi: 10.1029/2006GL027849

TURQUETY, S. HADJI-LAZARO, J. CLERBAUX, C. HAUGLUSTAINE, D. A. CLOUGH, S. A. CASSÉ, V. SCHLÜSSEL, P. MEGIE, G. 2004: Operational trace gas retrieval algorithm for the Infrared Atmospheric Sounding Interferometer Journal of Geophysical Research Vol. 109 No. 21 pp. D21301

VELDEN, C. S., C.M. HAYDEN, S. J. NIEMAN, W.P. MENZEL, S. WANZONG, and J.S. GOERSS, 1997: Upper-tropospheric winds derived from geostationary satellite water vapor observations. Bull. Amer. Meteor. So., 78, 173-195.

WAGNER, W., K. SCIPAL, C. PATHE, D. GERTEN, W. LUCHT, and B. RUDOLF (2003), Evaluation of the agreement between the first global remotely sensed soil moisture data with model and precipitation data. J. Geophys. Res., 108(D19), 4611, doi: 10.1029/2003JD003663.